

Detecting Intermediate-mass Black Holes Using Miniature Pulsar Timing Arrays in Globular Clusters

Xian Chen,^{1,2,*} Verónica Vázquez-Aceves,² Siyuan Chen,^{3,4} Kejia Lee,^{1,5,6,7} Yanjun Guo,^{5,4} and Kuo Liu^{3,4}

¹*Department of Astronomy, School of Physics, Peking University, 100871 Beijing, China*

²*Kavli Institute for Astronomy and Astrophysics at Peking University, 100871 Beijing, China*

³*Shanghai Astronomical Observatory, Chinese Academy of Sciences, 80 Nandan Road, Shanghai 200030, China*

⁴*State Key Laboratory of Radio Astronomy and Technology,*

A20 Datun Road, Chaoyang District, Beijing, 100101, P. R. China

⁵*National Astronomical Observatories, Chinese Academy of Sciences,*

A20 Datun Road, Chaoyang District, Beijing, 100101, P. R. China

⁶*Yunnan Astronomical Observatories, Chinese Academy of Sciences, Kunming 650216, Yunnan, P. R. China*

⁷*Beijing Laser Acceleration Innovation Center, Huairou, Beijing, 101400, P. R. China*

(Dated: July 14, 2025)

Theoretical models predict that intermediate-mass black holes (IMBHs) exist in globular clusters (GCs), but observational evidence remains elusive. Millisecond pulsars (MSPs), which are abundant in GCs and have served as precise probes for gravitational waves (GWs), offer a unique opportunity to detect potential IMBH binaries in GCs. Here, we consider the possibility of using multiple MSPs in a GC to form a miniature pulsar timing array (PTA), so as to take advantage of their correlated timing residuals to search for potential IMBH binaries in the same cluster. Our semi-analytical calculations reveal that nearby IMBH binaries around MSPs in GCs could induce microsecond-level timing residuals. In GCs like ω Centauri and M15, favorable configurations are found which could lead to the detection of binaries with mass ratios $q \gtrsim 0.1$ and orbital periods of a few days. We estimate that future higher-precision timing programs could achieve 100-nanosecond sensitivity, substantially expanding the searchable parameter space and establishing mini-PTAs as powerful detectors of IMBHs.

I. INTRODUCTION

Millisecond pulsars (MSPs) are highly stable rotators and can serve as precise probes for detecting spacetime distortions caused by gravitational waves (GWs) [1, 2]. By monitoring an array of MSPs in the Galactic field and analyzing correlations in their timing residuals, astronomers can detect stochastic GW backgrounds [3]. This method, known as the pulsar timing array (PTA) technique, recently led to the discovery of a possible signal of nanohertz GW background [4–8].

Globular clusters (GCs) are one of the primary locations where MSPs are found. Since the first GC pulsar detection [9], over 330 pulsars have been observed in these dense stellar systems [10]. Remarkably, more than 95% of these GC pulsars have spin periods shorter than 30 milliseconds (ms), a significantly higher fraction than their counterparts in the Galactic field. Many are isolated, lacking binary companions (e.g., [11, 12]). Recent GC pulsar discoveries have been made by major radio telescopes, including FAST [13–16], MeerKAT [17], GMRT [18], and Parkes [19, 20]. Future observations with the Square Kilometre Array (SKA) are projected to detect 100–300 pulsars in a comprehensive survey of approximately 150 Galactic GCs during its first phase, and the number of pulsars may grow to 3700 in the second phase of SKA observation [21].

GCs may also harbor a class of elusive objects known as intermediate-mass black holes (IMBHs), whose masses range from 10^2 to $10^5 M_\odot$. While the existence of IMBHs in GCs has long been predicted by theoretical models [22], robust observational evidence remains lacking (see reviews in [23, 24]). Nevertheless, both numerical N-body simulations (e.g., [25, 26]) and semi-analytical Monte-Carlo models (e.g., [27]) suggest that IMBHs in GCs could produce two distinct types of GW sources. (i) An IMBH in a GC, through frequent gravitational interactions with surrounding stars, could capture the most massive object in the cluster, likely a stellar-mass black hole (BH) of $\sim 10 M_\odot$ [28, 29], and form a binary of intermediate mass ratio ($10^{-4} \lesssim q \lesssim 10^{-2}$). Such a binary can persist for a significant fraction of the cluster’s lifetime [30, 31] before being disrupted by stellar interactions, replaced by another stellar companion, or driven to merger by GW radiation [32, 33]. (ii) Two IMBHs may exist in the same GC, due to either efficient formation of very massive stars via stellar collisions [34] or mergers of GCs [35]. In either case, the two IMBHs could quickly form a binary and, depending on the mass ratio and orbital eccentricity, survive for hundreds of millions of years before merging due to GW radiation [36–38]. In the following, we will refer to the aforementioned two types of GW sources as the “IMBH binaries”.

The potential coexistence of MSPs and IMBH binaries within GCs has motivated the calculation of MSP timing residuals induced by nearby GW sources. The initial calculations focused on binary neutron stars and stellar-origin BHs as GW sources [39, 40] and estimated that

* xian.chen@pku.edu.cn

the timing residual could be as large 100 nano-seconds (ns) [41]. These earlier studies, as well as the later more robust calculations [42–44], also clarified a crucial difference between the current scenario and the conventional PTA technique. In the traditional PTA setup, pulsars are far away from the GW sources so that pulsar emissions propagate at a constant angle relative to the GW wave vector. However, in the context of GCs, this assumption breaks down due to the proximity of the MSPs to the potential GW sources. More recently, Jenet et al. [45] developed a simplified framework to calculate this “near-field” effect, demonstrating that the continuous GWs from IMBH binaries can induce timing residuals with amplitudes as large as 500 ns, well within the detection capabilities of modern radio telescopes. Even if IMBH mergers produce short GW bursts, their imprint on timing residuals remains detectable when MSPs and IMBH binaries coexist in the same GCs [46].

While previous studies have primarily focused on the timing residuals of individual MSPs, it is important to note that variations in a single pulsar’s timing residual alone cannot conclusively confirm the presence of a GW source in the GC. Such variations could alternatively arise from the pulsar being part of a binary system (e.g., [47]). Traditionally, definitive evidence requires observing the characteristic angular correlation between timing residuals of different MSPs (the Hellings-Downs curve [3]). However, this standard approach faces challenges when applied to GC MSPs, as current observations only provide the two-dimensional projected sky positions of MSPs, lacking the full directional information needed for conventional correlation analysis. Nevertheless, in principle, the timing residuals of different MSPs within the same GC should exhibit correlations due to their shared proximity to a potential GW source. The key uncertainty is whether the correlations are prominent enough for detection.

To address this question, we first derive simplified semi-analytical expressions for near-field timing residuals based on Ref. [45], explicitly characterizing the dependence on the projected distance between the MSP and the IMBH binary. Next, we evaluate the sensitivity of a compact array of MSPs in a GC, functioning as a miniature PTA, for detecting potential IMBH binaries within the same GC. These theoretical developments are timely given the recent new evidence for IMBHs in ω Centauri [48] and M15 [49], coupled with ongoing discoveries and monitoring of new MSPs in these clusters [13, 19, 20].

II. THEORY

A. Timing residual

Figure 1 illustrates the system of our interest (also see Fig. 1 in Ref. [45]). Both the GW source and the pulsar reside in a GC which is far from the observer ($r_e \ll r_o$). The GW source is a binary composed of an IMBH of

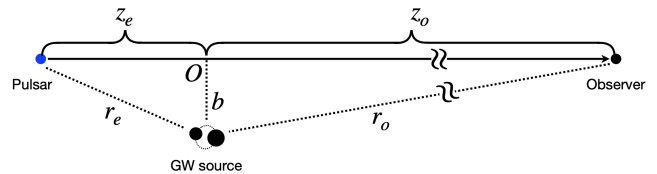


FIG. 1: System configuration and definition of the parameters (also see Ref. [45]).

mass m_1 and a smaller BH of mass m_2 . The impact parameter b quantifies the minimum distance between the GW source and the observer’s line of sight to the pulsar. We are particularly interested in the case where $b \ll r_e$. We define the z axis to be the direction from the pulsar to the observer (solid line with arrow). In this direction, the pulsar’s emission intersects with the GWs from the binary source, with the angle between the electromagnetic and GW vectors varying at each intersection point. This angular variation distinguishes our scenario from the conventional PTA setup.

GW perturbs the spacetime at the pulsar, the observer, and in between. As a result, the time at which a pulse arrives at the observer differs from that in flat spacetime by an amount of

$$R(t) = \int_0^t \frac{\nu_0 - \nu(t')}{\nu_0} dt' \quad (1)$$

[2, 50], where $\nu_0 = -K_\mu^e V^{e\mu}$ is the intrinsic spin frequency in the rest frame of the pulsar, and $\nu = -K_\mu^o V^{o\mu}$ is the apparent spin frequency measured by the observer. Here V^μ denotes time-like four velocity, K_μ is the dual to photon four vector, and the superscript o denotes a quantity defined at the observer while e at the emitter (pulsar). The resulting $R(t)$ is also known as the “timing residual”.

We notice that if the pulsar or the observer is moving at a constant velocity relative to the GW source, the equations derived below remain valid except for a modification of the frequencies by a constant Doppler factor. Since the velocity is typically negligible relative to the speed of light, we will ignore it in our calculation. If the pulsar is accelerating due to the pulling by other stars, the sum of these accelerations may cause the apparent period of the pulsar to vary. However, the magnitude of this acceleration is normally smaller than 10^{-7} m s^{-2} [51] and the timescale for the acceleration to change is typically $10^2 - 10^3$ years [52, 53]. Therefore, during an observational period of, say, ten years, the second time derivative of the pulsar period is too small to detect [52] unless rare close encounters happen [53]. As a result, the acceleration induces almost a constant period derivative, which could be absorbed into the parameters of a timing model and elude detection [52]. For this reason as well as for simplicity, we could neglect acceleration in the current work.

To facilitate the later calculations, we use bars to de-

note the physical quantities when there is no GW, so that $-\bar{K}_\mu \bar{V}^{e\mu} = -\bar{K}_\mu \bar{V}^{o\mu} = \nu_0$. When GW is introduced, we can expand the four vectors to linear order in perturbation, $V^{o\mu} = \bar{V}^{o\mu} + \delta V^{o\mu}$ and $K_\mu^o = \bar{K}_\mu + \delta K_\mu^o$, and then find that

$$\frac{\nu_0 - \nu(t)}{\nu_0} = \frac{\bar{K}_\mu \delta V^{o\mu} + \bar{V}^{o\mu} \delta K_\mu^o}{\bar{K}^t c} \simeq \frac{\delta K_t^o}{\bar{K}^t}, \quad (2)$$

where $\bar{K}^t = \nu_0/c$. In the last equation, we neglect the term $\bar{K}_\mu \delta V^{o\mu}$, which is proportional to the GW amplitude at the observer and hence proportional to $1/r_o$. While the remaining term $\bar{V}^{o\mu} \delta K_\mu^o$ is proportional to $1/\min(r_e, b)$, therefore bigger than the previous one by a factor of $10^4 - 10^5$ for typical GC systems.

To calculate δK_t^o in Equation (2), we assume that the GW strain tensor $h_{\mu\nu}$ is small relative to the Minkowski metric $\eta_{\mu\nu} = \text{diag}(-1, 1, 1, 1)$ and subtract the two null geodesic equations with and without GW. Then to linear order of $h_{\mu\nu}$ we derive

$$\frac{d\delta K_t}{d\lambda} = \frac{1}{2} h_{\mu\nu,t} \bar{K}^\mu \bar{K}^\nu, \quad (3)$$

where $h_{\mu\nu,t}$ denotes the partial derivative $(\partial h_{\mu\nu}/\partial t)/c$, and λ is an affine parameter for which we choose $\lambda = z/\bar{K}^t$. Integrating the above equation from the pulsar to the observer, and noticing that $\bar{K}^\mu = (\nu_0/c, 0, 0, \nu_0/c)$, we find

$$\frac{\delta K_t^o}{\bar{K}^t} = \frac{\delta K_t^e}{\bar{K}^t} + \int_{z_e}^{z_o} \frac{h_{tt,t} + h_{zz,t} + 2h_{tz,t}}{2} dz. \quad (4)$$

The first term on the right-hand side is a ‘‘pulsar term’’ caused by the the GWs interacting with the pulsar. The second term results from the interaction between GW and photon.

Now the task left is to express δK_t^e in terms of $h_{\mu\nu}$. We start from the fact that in the rest frame of the pulsar, the spin frequency remains ν_0 . Mathematically, this means $-(\bar{V}^{e\mu} + \delta V^{e\mu})(\bar{K}_\mu^e + \delta K_\mu^e) = \nu_0$. Assuming that the pulsar is not moving, i.e., $\bar{V}^{e\mu} = (c, 0, 0, 0)$, to linear order we can write

$$\delta K_t^e = -\frac{\nu_0}{c^2} (\delta V_t^e + \delta V_z^e). \quad (5)$$

Applying the geodesic equation for the pulsar,

$$\frac{d\delta V_\alpha}{d\tau} = \frac{1}{2} h_{\mu\nu,\alpha} \bar{V}^\mu \bar{V}^\nu = \frac{c^2}{2} h_{tt,\alpha}, \quad (6)$$

we finally find

$$\frac{\delta K_t^e}{\bar{K}^t} = -c \int_0^t \frac{h_{tt,t} + h_{tt,z}}{2} dt'. \quad (7)$$

Notice that Equation (7) is integrated over time, while the integration in Equation (4) is performed with respect to space.

B. GW strain

Now we evaluate the GW strain $h_{\mu\nu}$ at the position \mathbf{r} and the local time t . We follow Ref. [45] and use the formula

$$h_{\mu\nu}(t, \mathbf{r}) = \frac{4G}{c^4} \int \frac{\bar{T}_{\mu\nu}(t - |\mathbf{r} - \mathbf{r}'|/c, \mathbf{r}')}{|\mathbf{r} - \mathbf{r}'|} d^3 \mathbf{r}', \quad (8)$$

where $\bar{T}_{\mu\nu}$ is the trace-reversed stress energy tensor for the GW source, \mathbf{r}' refers to the source position, and notice that the result is not in transverse-traceless gauge. Because $r' = |\mathbf{r}'|$ is comparable to the size of the GW source, and in our scenario much smaller than $r = |\mathbf{r}|$, we can expand $|\mathbf{r} - \mathbf{r}'|$ to the order of $O(r')$ and rewrite the strain as

$$h_{\mu\nu}(t, \mathbf{r}) \simeq \frac{4G}{rc^4} \int \left(\bar{T}_{\mu\nu} + \bar{T}_{\mu\nu} \frac{\mathbf{n} \cdot \mathbf{r}'}{r} + \frac{\mathbf{n} \cdot \mathbf{r}'}{c} \frac{\partial \bar{T}_{\mu\nu}}{\partial t} \right) d^3 \mathbf{r}', \quad (9)$$

where $\bar{T}_{\mu\nu}(t - r/c, \mathbf{r}')$ and $\mathbf{n} = \mathbf{r}/r$. The second term in the integrand is smaller than the first one by a factor of r'/r , and hence we neglect it in the later calculation. The third term is also negligible in the low-velocity limit, which applies to our GW source.

Therefore, we can keep only the first term in the integrand of Equation (9). Then applying the standard perturbative technique in the weak-field, low-velocity limit [54], we derive

$$h_{tt} = \frac{2G}{rc^4} \left(Mc^2 + \frac{\ddot{Q}_{xx} + \ddot{Q}_{yy} + \ddot{Q}_{zz}}{2} \right), \quad (10)$$

$$h_{zz} = \frac{2G}{rc^4} \left(Mc^2 - \frac{\ddot{Q}_{xx} + \ddot{Q}_{yy} - \ddot{Q}_{zz}}{2} \right), \quad (11)$$

$$h_{tz} = -\frac{4GP^z}{rc^4} = 0, \quad (12)$$

where $M = \int (T^{00}/c^2) d^3 \mathbf{r}' = m_1 + m_2$ is the total mass of the binary GW source, $Q_{ij} = Q^{ij} = \int T^{00} x'^i x'^j d^3 \mathbf{r}'$ is the mass quadrupole moment of the source, and $P^z = \int T^{0z} d^3 \mathbf{r}'$ is the linear momentum in the z direction. For the convenience of later calculation, we define $Q \equiv Q_{xx} + Q_{yy} + Q_{zz}$.

When using Equations (10)-(12), one has to treat Q_{ij} as a function of the retarded time $t_*(t, z) = t - (z_o - z)/c - \sqrt{z^2 + b^2}/c$, so that t corresponds to the time when the pulse arrives at the observer. Consequently, both Q_{ij} and $r = \sqrt{z^2 + b^2}$ are functions of z , so we can derive the following useful relation

$$h_{tt,z} = -\frac{z h_{tt}}{z^2 + b^2} + h_{tt,t} \left(1 - \frac{z}{r} \right). \quad (13)$$

Using this relation, as well as Equations (2), (4), and (7), we find that

$$\begin{aligned} \frac{\nu_0 - \nu(t)}{\nu_0} &= \int_0^t \frac{z_e h_{tt}}{2r_e^2} c dt' - \int_0^t \frac{h_{tt,t}}{2} \left(2 - \frac{z_e}{r_e} \right) c dt' \\ &\quad + \int_{z_e}^{z_o} \frac{h_{tt,t} + h_{zz,t}}{2} dz. \end{aligned} \quad (14)$$

C. Semi-analytical expressions

Further calculation of $R(t)$ requires some specification of the system. Without loss of generality, we assume that the GW source, i.e., the IMBH binary, is circular with an orbital angular frequency of ω_b . The resulting GW radiation is monochromatic with a frequency of ω_b/π . Since GWs from eccentric binaries can be decomposed into a series of harmonics [55], our analysis of single harmonic components provides a foundation for future studies of eccentric binary GW sources.

Motivated by observations, we consider an IMBH of a mass of $m_1 = (10^3 - 10^4)M_\odot$, and we assume that it resides at the center of a GC. The companion is a BH of equal or smaller mass, so that the mass ratio of the binary is $q = m_2/m_1 \leq 1$. The semimajor axis of the binary orbit is typically $a = (10^2 - 10^7)r_g$, where $r_g = Gm_1/c^2$ is the gravitational radius of the IMBH. Therefore, the orbital period is

$$P = 2\pi \left(\frac{a^3}{GM} \right)^{1/2} \simeq \frac{113 \text{ days}}{(1+q)^{1/2}} \left(\frac{m_1}{10^4 M_\odot} \right) \left(\frac{a}{10^5 r_g} \right)^{3/2} \quad (15)$$

and due to GW radiation [55] the binary has a lifetime of

$$T_{\text{gw}} = \frac{a}{4|\dot{a}|} = \frac{5a^4}{256cr_g^3q(1+q)} \quad (16)$$

$$\simeq \frac{3.05 \times 10^9 \text{ yrs}}{q(1+q)} \left(\frac{m_1}{10^4 M_\odot} \right) \left(\frac{a}{10^5 r_g} \right)^4. \quad (17)$$

Given such a circular binary system with a reduced mass of $\mu = m_1 m_2 / (m_1 + m_2)$ and semimajor axis of a , the mass quadrupole moment is of the order of $\sim \mu a^2 \cos(2\omega_b t + \phi)$, where the exact coefficient and the phase (ϕ) depend on the orientation of the binary. Since a summation of sinusoidal functions of the same frequency remains a sinusoidal function except for a different coefficient and an additional phase factor, we can regard the mass quadrupole moments and their linear combinations as functions of $\cos(2\omega_b t + \phi)$. Their time derivatives can be derived accordingly, e.g., $\ddot{Q} \sim -4\omega_b^2 \mu a^2 \cos(2\omega_b t + \phi)$.

Given the above specification, we can integrate the first term in Equation (14). In the integrand, the term containing M/r_e does not vary with time; therefore, the integral can be absorbed into a constant Doppler shift in the timing model. Integrating the rest time-dependent parts gives

$$\frac{z_e G}{2r_e^3 c^3} \int_0^t \ddot{Q} dt' = A_1 \left(\frac{\omega_b \mu a^2 z_e G}{r_e^3 c^3} \right) \cos(2\omega_b t + \phi_1) \quad (18)$$

$$= \frac{A_1 q}{(1+q)^{1/2}} \sqrt{\frac{a}{r_g}} \left(\frac{z_e}{r_e} \right) \left(\frac{r_g}{r_e} \right)^2 \cos(2\omega_b t + \phi_1) \quad (19)$$

where the coefficient A_1 is of order unity, and the phase ϕ_1 depends on the orientation of the binary as well as the initial position of the companion BH. If we use $M =$

$10^4 M_\odot$, $q \simeq 1$, $z_e \sim r_e$, $a \sim 10^5 r_g$, and $r_e \sim 1$ pc as the fiducial values, we find that the magnitude of $(\nu_0 - \nu)/\nu_0$ contributed by the first term in Equation (14) is about 10^{-17} . To estimate the corresponding timing residual, we notice that $1/(2\omega_b) \sim 10^6$ s in the fiducial model. Therefore, $R(t)$ is of the order of 10^{-11} s due to the first term, which is too small for the current radio telescopes to detect.

As for the second term in Equation (14), the integration gives

$$\frac{G\ddot{Q}}{2r_e c^4} \left(\frac{z_e}{r_e} - 2 \right) = A_2 \left(\frac{2qr_g^2}{ar_e} \right) \left(\frac{z_e}{r_e} - 2 \right) \times \cos(2\omega_b t + \phi_2). \quad (20)$$

In our fiducial model, it is a factor of

$$\frac{2r_e r_g^{1/2}}{(1+q)^{1/2} a^{3/2}} \sim 10^2 \quad (21)$$

times bigger than the first term in Equation (14). The corresponding $R(t)$ reaches a few ns, but still too small to detect.

Finally, we integrate the third term in Equation (14). With Equations (10) and (11), the integral reduces to

$$\int_{z_e}^{z_o} \frac{G\ddot{Q}_{zz}}{rc^5} dz = A_3 \left(\frac{8G\mu a^2 \omega_b^3}{c^5} \right) H(t, z) \Big|_{z_e}^{z_o}, \quad (22)$$

where

$$H(t, z) = \int^z \frac{\sin(2\omega_b t_* + \phi_3)}{\sqrt{z'^2 + b^2}} dz' \quad (23)$$

$$= \cos[2\omega_b(t - z_o/c + \phi_3)] \text{Si} \left[\frac{\sqrt{z^2 + b^2} - z}{c/(2\omega_b)} \right] - \sin[2\omega_b(t - z_o/c + \phi_3)] \text{Ci} \left[\frac{\sqrt{z^2 + b^2} - z}{c/(2\omega_b)} \right], \quad (24)$$

and

$$\text{Si}(x) = \int^x \frac{\sin(x')}{x'} dx', \quad (25)$$

$$\text{Ci}(x) = \int^x \frac{\cos(x')}{x'} dx'. \quad (26)$$

We notice that the fraction in the parentheses of Equation (22),

$$\frac{8G\mu a^2 \omega_b^3}{c^5} = 8q(1+q)^{1/2} \left(\frac{r_g}{a} \right)^{5/2}, \quad (27)$$

is bigger than the fraction in Equation (18) by a factor of

$$8(1+q) \frac{r_g r_e^3}{a^3 z_e} \sim 10^4 \quad (28)$$

in our fiducial model.

Therefore, the third term on the right-hand side of Equation (14) can potentially dominate the first two terms. This term originates from the interaction between electromagnetic pulses and GWs. Since the integral depends on $H(t, z)$ which is a sinusoidal function of $2\omega_b t$, we can integrate it with respect to t according to Equation (1), and estimate the magnitude of the timing residual as

$$\begin{aligned} \frac{R(t)}{\cos(2\omega_b t + \phi)} &\sim \left(\frac{4G\mu a^2 \omega_b^2}{c^5} \right) \sqrt{(\Delta\text{Ci})^2 + (\Delta\text{Si})^2} \\ &\simeq 2\mu\text{s} \sqrt{(\Delta\text{Ci})^2 + (\Delta\text{Si})^2} \left(\frac{m_1 q}{10^4 M_\odot} \right) \left(\frac{a}{10^5 r_g} \right)^{-1} \end{aligned} \quad (30)$$

where ΔCi (ΔSi) represents the difference between the two cosine (sine) integrals evaluated at the pulsar and the observer positions. These differences arise from the calculation of $H(t, z)|_{z_e}^{z_o}$ in Equation (22).

Interestingly, we find that the value of $\sqrt{(\Delta\text{Ci})^2 + (\Delta\text{Si})^2}$ is of the order of unity for our fiducial GC-MSP systems. This is because the value of the term $(\sqrt{z_e^2 + b^2} - z_e)/(c/2\omega_b)$ in the brackets of Equation (24) is typically $\gg 1$ at the emitter ($z = z_e$) and, more importantly, $\ll 1$ at the observer ($z = z_o \sim 10$ kpc). The notably small value observed at $z = z_o$ is primarily due to the small impact parameter b , which satisfies the condition $b/z_o \ll 1$. As a result, both $|\Delta\text{Ci}|$ and $|\Delta\text{Si}|$ turn out to be of order unity. Another interesting and useful result is that in real GC systems where $(\sqrt{z_e^2 + b^2} - z_e)/(c/2\omega_b) \gg 1$ is often satisfied, neither $|\Delta\text{Ci}|$ nor $|\Delta\text{Si}|$ is sensitive to the sign or magnitude of z_e . In this case, the timing residual $R(t)$ only depends on the projected distance b between the pulsar and the IMBH binary, making observational constraints more feasible.

III. EXAMPLES

The coefficient of $2\mu\text{s}$ in Equation (30) puts the timing residual in a potentially detectable range. In the following, we showcase two real GC-MSP systems to highlight the detectability of the timing residual.

ω Cen is the most massive GC in the Galaxy and one of the best observationally studied due to its closeness to the earth (5.2 kpc). It has been considered a prime candidate for hosting an IMBH in its core [24]. Recent discovery of several fast-moving stars within its central 0.1 pc further suggests that the IMBH should be $\gtrsim 10^4 M_\odot$. However, the distribution and acceleration of the MSPs in ω Cen seems more consistent with an extended central mass, and the corresponding models have put an upper limit of about $6 \times 10^3 M_\odot$ on the IMBH mass [56].

Given the current theoretical and observational uncertainties, we assume $m_1 + m_2 = 10^4 M_\odot$, as well as $b = 1$ pc and $z_e = -1$ pc to account for a typical MSP in ω Cen [19]. The resulting timing residual as a function of the binary semimajor axis a and mass ratio q is shown

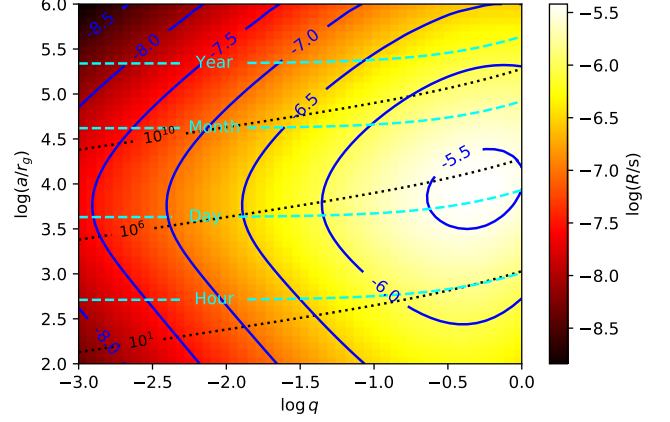


FIG. 2: Timing residual (color map and blue contours) for a MSP in ω Cen, where we have assumed an impact parameter of $b = 1$ pc for the MSP and a total mass of $m_1 + m_2 = 10^4 M_\odot$ for the binary GW source. The four cyan dashed curves correspond to orbital periods ranging from 1 year to 1 hour, and the black dotted curves correspond to three GW radiation timescales, $T_{\text{gw}} = 10^{10}$, 10^6 , and 1 yr, for the binary.

in Figure 2. We find that $R(t)$ reaches a maximum value of about $3\mu\text{s}$ when the two BHs are relatively equal in mass ($q \gtrsim 0.3$) and on an orbit of a period of about a few days. This maximum is comparable to the coefficient $2\mu\text{s}$, indicating that $H(t, z)|_{z_e}^{z_o} \sim 1$.

Current observations of the MSPs in ω Cen have achieved a timing precision of $\sim 10 \mu\text{s}$ with an integration time of ~ 1 hour [20]. If the same pulsars are observed repeatedly, accumulating $N \sim 10^2$ timing residual measurements, it becomes feasible to detect a residual as small as $\sim 1\mu\text{s}$ (see Section IV). According to Figure 2, those GW sources resulting in $R > 1\mu\text{s}$ mostly have $q > 0.1$ and distribute in a broad semimajor-axis range. The widest binaries among them have a lifetime of 10^{10} yrs, increasing the probability that such binaries may exist in ω Cen today.

M15 is a core-collapse GC located at a distance of 10 kpc from the earth. Current stellar kinematic models remain inconclusive regarding the existence and mass of an IMBH in M15, with possible mass estimates ranging from about $4000 M_\odot$ to as small as $500 M_\odot$ [49, 57, 58]. Meanwhile, 15 pulsars have been discovered in M15 where more than half of them have a spin period shorter than $30\mu\text{s}$. In particular, a few MSPs reside within a projected distance of 0.1 pc from the center of the GC, and recent timing of them has achieved a precision of about $20\mu\text{s}$ [13].

Therefore, we assume a total mass of $m_1 + m_2 = 3 \times 10^3 M_\odot$ for the IMBH binary in M15 [57], and $b = 0.1$ pc and $z_e = -1$ pc for the MSP [13]. The resulting timing residual as a function of the binary semimajor axis a and mass ratio q is shown in Figure 3. Now the peak of $R(t)$ is higher than in the previous case, exceeding

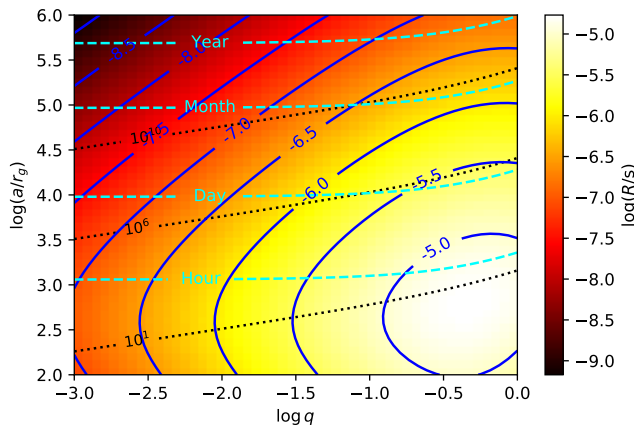


FIG. 3: Same as Figure 2 but for M15, where we have assumed $b = 0.1$ pc and $m_1 + m_2 = 3 \times 10^3 M_\odot$.

$10\mu\text{s}$. But the location of the peak in the $q - a$ diagram shifts to smaller a/r_g . Because the corresponding orbital period is shorter than an hour, detecting such a GW source requires high observational cadence, which is challenging with the current telescopes. However, a fraction of the parameter space above the curve of $P = 1$ day still allows $R(1) > 1\mu\text{s}$. Here, IMBH binaries have a lifetime between 10^6 and 10^9 years (see black dotted lines). Whether or not such binaries exist can be tested by timing the MSPs in M15.

IV. DETECTABILITY

Now we discuss how to find a signal like that described in Equation (30) from noisy timing data. Suppose the noise $n(t)$ follows a Gaussian distribution with zero mean $\langle n \rangle = 0$ and has a variance of $\text{Var}(n) = \langle n^2 \rangle = \sigma^2$. In the null hypothesis, when there is no signal, the data $d(t_i)$ will contain pure noise, where t_i denotes the time when the i th timing residual is measured. If one uses a template $R(t) = \cos(\tilde{\omega}t_i + \tilde{\phi})$ to do a matched-filtering analysis, i.e., calculating the overlap

$$T_n = \sum_{i=1}^N d(t_i)R(t_i), \quad (31)$$

the result will have a mean value of $\bar{T}_n = 0$ with a variance of $\text{Var}(T_n) = N\sigma^2/2$.

In the alternative hypothesis, if there is a sinusoidal signal of amplitude A , angular frequency ω , and phase ϕ , the data will become $d(t_i) = s(t_i) + n(t_i)$, where $s(t_i) = A \cos(\omega t_i + \phi)$ is the signal. Notice that we are interested in the case $A \ll \sigma$. Now the result of Equation (31) will depend on the choices of $\tilde{\omega}$ and $\tilde{\phi}$. But one can experiment with different $\tilde{\omega}$ and $\tilde{\phi}$ to look for the maximum, which we denote as T_{max} . In the ideal situation, that the number of measurements N is sufficiently large, and the time span of the data covers at least

one GW period $2\pi/\omega$, the maximum should be found at $\tilde{\omega} = \omega$ and $\tilde{\phi} = \phi$, and the corresponding value is

$$T_{\text{max}} = \sum_{i=1}^N A \cos^2(\omega t_i + \phi) + \sum_{i=1}^N n_i \cos(\omega t_i + \phi). \quad (32)$$

The mean and the variance of T_{max} are, respectively,

$$\bar{T}_{\text{max}} \simeq \frac{NA}{2}, \quad (33)$$

$$\text{Var}(T_{\text{max}}) \simeq \frac{NA^2}{8} + \frac{N\sigma^2}{2} \simeq \frac{N\sigma^2}{2}, \quad (34)$$

where, again, we have assumed a long observation duration and a large number of timing residual measurements, so that those terms containing $\cos(\omega t_i + \phi)$, $\cos(2\omega t_i + 2\phi)$, $\cos(3\omega t_i + 3\phi)$, and $\cos(4\omega t_i + 4\phi)$ all vanish upon ensemble averaging.

Now we propose a detection threshold based on two considerations. (1) Signal presence condition: If a true signal exists, T_{max} should exceed $\bar{T}_{\text{max}} - 1.64\sqrt{\text{Var}(T_{\text{max}})}$ with 95% probability. (2) Statistical significance condition: To limit false alarms to less than 5%, we require $T_{\text{max}} > \bar{T}_n + 1.64\sqrt{\text{Var}(T_n)}$. The combined threshold is therefore $\bar{T}_{\text{max}} - 1.64\sqrt{\text{Var}(T_{\text{max}})} > \bar{T}_n + 1.64\sqrt{\text{Var}(T_n)}$, which corresponds to

$$A \gtrsim 4.65\sigma/\sqrt{N}. \quad (35)$$

Signals with this amplitude can be reliably distinguished from background noise with high probability.

Current observations of MSPs in GCs are approaching a timing precision (weighted rms) of $\sigma \simeq 10\mu\text{s}$ as well as a total number of 100 measurements for a single MSP [13, 20]. They will allow us to detect GWs with an amplitude of $A \gtrsim 4.7\mu\text{s}$. Such a sensitivity corresponds to a contour level of about -5.3 in Figures 2 and 3. Interestingly, such contours will enclose a small, but non-zero fraction of the parameter space. Therefore, we would be able to test the existence of IMBH binaries in GCs by timing even a single MSP.

More importantly, as we have mentioned earlier, multiple MSPs are often found in a single GC, and the number N_p could be as large as $O(10)$. According to our analysis of the matched-filtering method, using the timing data of all the MSPs with similar timing precision will further improve the sensitivity by a factor of $\sqrt{N_p}$. It is worth mentioning that by substantially increasing the timing precision (σ) or the number of MSPs (N_p), a sensitivity of $A \sim O(10^2)$ ns may be reached in the future. Then a significantly larger portion of the parameter space shown in Figures 2 and 3 for potential IMBH binaries could become accessible via pulsar timing. The envisioned mini-PTA will then serve as an even more powerful probe for IMBHs.

ACKNOWLEDGMENTS

This work is supported by the National Key Research and Development Program of China (Grant No. SQ2024YFC220046) and the National Natural Science Foundation of China (Grant No. 12473037). KJL thanks the Xplorer Prize for the support.

-
- [1] M. V. Sazhin, Opportunities for detecting ultralong gravitational waves, *Sov. Astron.* **22**, 36 (1978).
- [2] S. Detweiler, Pulsar timing measurements and the search for gravitational waves, *Astrophys. J.* **234**, 1100 (1979).
- [3] R. W. Hellings and G. S. Downs, Upper limits on the isotropic gravitational radiation background from pulsar timing analysis., *Astrophys. J. Lett.* **265**, L39 (1983).
- [4] G. Agazie, M. F. Alam, A. Anumalapudi, A. M. Archibald, Z. Arzoumanian, P. T. Baker, L. Blecha, V. Bonidie, A. Brazier, P. R. Brook, S. Burke-Spolaor, B. Bécsy, C. Chapman, M. Charisi, S. Chatterjee, T. Cohen, J. M. Cordes, N. J. Cornish, F. Crawford, H. T. Cromartie, K. Crowder, M. E. Decesar, P. B. Demorest, T. Dolch, B. Drachler, E. C. Ferrara, W. Fiore, E. Fonseca, G. E. Freedman, N. Garver-Daniels, P. A. Gentile, J. Glaser, D. C. Good, K. Gültekin, J. S. Hazboun, R. J. Jennings, C. Jessup, A. D. Johnson, M. L. Jones, A. R. Kaiser, D. L. Kaplan, L. Z. Kelley, M. Kerr, J. S. Key, A. Kuske, N. Laal, M. T. Lam, W. G. Lamb, T. J. W. Lazio, N. Lewandowska, Y. Lin, T. Liu, D. R. Lorimer, J. Luo, R. S. Lynch, C.-P. Ma, D. R. Madison, K. Maraccini, A. McEwen, J. W. McKee, M. A. McLaughlin, N. McMann, B. W. Meyers, C. M. F. Mingarelli, A. Mitridate, C. Ng, D. J. Nice, S. K. Ocker, K. D. Olum, E. Panciu, T. T. Pennucci, B. B. P. Perera, N. S. Pol, H. A. Radovan, S. M. Ransom, P. S. Ray, J. D. Romano, L. Salo, S. C. Sardesai, C. Schmiedekamp, A. Schmiedekamp, K. Schmitz, B. J. Shapiro-Albert, X. Siemens, J. Simon, M. S. Siwek, I. H. Stairs, D. R. Stinebring, K. Stovall, A. Susobhanan, J. K. Swiggum, S. R. Taylor, J. E. Turner, C. Unal, M. Vallisneri, S. J. Vigeland, H. M. Wahl, Q. Wang, C. A. Witt, O. Young, and Nanograv Collaboration, The NANOGrav 15 yr Data Set: Observations and Timing of 68 Millisecond Pulsars, *Astrophys. J. Lett.* **951**, L9 (2023), [arXiv:2306.16217 \[astro-ph.HE\]](#).
- [5] EPTA Collaboration, InPTA Collaboration, J. Antoniadis, P. Arumugam, S. Arumugam, S. Babak, M. Bagchi, A. S. Bak Nielsen, C. G. Bassa, A. Bathula, A. Berthureau, M. Bonetti, E. Bortolas, P. R. Brook, M. Burgay, R. N. Caballero, A. Chalumeau, D. J. Champion, S. Chanlaridis, S. Chen, I. Cognard, S. Dandapat, D. Deb, S. Desai, G. Desvignes, N. Dhanda-Batra, C. Dhivedi, M. Falxa, R. D. Ferdman, A. Franchini, J. R. Gair, B. Goncharov, A. Gopakumar, E. Graikou, J. M. Grießmeier, L. Guillemot, Y. J. Guo, Y. Gupta, S. Hisano, H. Hu, F. Iraci, D. Izquierdo-Villalba, J. Jang, J. Jawor, G. H. Janssen, A. Jessner, B. C. Joshi, F. Karreem, R. Karuppusamy, E. F. Keane, M. J. Keith, D. Kharbanda, T. Kikunaga, N. Kolhe, M. Kramer, M. A. Krishnakumar, K. Lackeos, K. J. Lee, K. Liu, Y. Liu, A. G. Lyne, J. W. McKee, Y. Maan, R. A. Main, M. B. Mickaliger, I. C. Nițu, K. Nobleson, A. K. Paladi, A. Parthasarathy, B. B. P. Perera, D. Perrodin, A. Petiteau, N. K. Porayko, A. Possenti, T. Prabu, H. Quelquejay Leclere, P. Rana, A. Samajdar, S. A. Sanidas, A. Sesana, G. Shaifullah, J. Singha, L. Speri, R. Spiewak, A. Srivastava, B. W. Stappers, M. Surnis, S. C. Susarla, A. Susobhanan, K. Takahashi, P. Tarafdar, G. Theureau, C. Tiburzi, E. van der Wateren, A. Vecchio, V. Venkatraman Krishnan, J. P. W. Verbiest, J. Wang, L. Wang, and Z. Wu, The second data release from the European Pulsar Timing Array. III. Search for gravitational wave signals, *Astron. Astrophys.* **678**, A50 (2023), [arXiv:2306.16214 \[astro-ph.HE\]](#).
- [6] D. J. Reardon, A. Zic, R. M. Shannon, G. B. Hobbs, M. Bailes, V. Di Marco, A. Kapur, A. F. Rogers, E. Thrane, J. Askew, N. D. R. Bhat, A. Cameron, M. Curylo, W. A. Coles, S. Dai, B. Goncharov, M. Kerr, A. Kulkarni, Y. Levin, M. E. Lower, R. N. Manchester, R. Mandow, M. T. Miles, R. S. Nathan, S. Osłowski, C. J. Russell, R. Spiewak, S. Zhang, and X.-J. Zhu, Search for an Isotropic Gravitational-wave Background with the Parkes Pulsar Timing Array, *Astrophys. J. Lett.* **951**, L6 (2023), [arXiv:2306.16215 \[astro-ph.HE\]](#).
- [7] H. Xu, S. Chen, Y. Guo, J. Jiang, B. Wang, J. Xu, Z. Xue, R. N. Caballero, J. Yuan, Y. Xu, J. Wang, L. Hao, J. Luo, K. Lee, J. Han, P. Jiang, Z. Shen, M. Wang, N. Wang, R. Xu, X. Wu, R. Manchester, L. Qian, X. Guan, M. Huang, C. Sun, and Y. Zhu, Searching for the Nano-Hertz Stochastic Gravitational Wave Background with the Chinese Pulsar Timing Array Data Release I, *Research in Astronomy and Astrophysics* **23**, 075024 (2023), [arXiv:2306.16216 \[astro-ph.HE\]](#).
- [8] M. T. Miles, R. M. Shannon, D. J. Reardon, M. Bailes, D. J. Champion, M. Geyer, P. Gitika, K. Grunthal, M. J. Keith, M. Kramer, A. D. Kulkarni, R. S. Nathan, A. Parthasarathy, J. Singha, G. Theureau, E. Thrane, F. Abbate, S. Buchner, A. D. Cameron, F. Camilo, B. E. Moreschi, G. Shaifullah, M. Shamohammadi, A. Possenti, and V. V. Krishnan, The MeerKAT Pulsar Timing Array: the first search for gravitational waves with the MeerKAT radio telescope, *Mon. Not. R. Astron. Soc.* **536**, 1489 (2025), [arXiv:2412.01153 \[astro-ph.HE\]](#).
- [9] A. G. Lyne, A. Brinklow, J. Middleditch, S. R. Kulkarni, and D. C. Backer, The discovery of a millisecond pulsar in the globular cluster M28, *Nature (London)* **328**, 399 (1987).
- [10] Pulsars in GCs: <https://www3.mpifr-bonn.mpg.de/staff/pfreire/GCpsr.html>.
- [11] D.-J. Yin, L.-Y. Zhang, B.-D. Li, M.-H. Li, L. Qian, and Z. Pan, The Analyses of Globular Cluster Pulsars and Their Detection Efficiency, *Research in Astronomy and Astrophysics* **23**, 055012 (2023), [arXiv:2303.09710 \[astro-ph.HE\]](#).

- ph.HE].
- [12] D. Yin, L.-y. Zhang, L. Qian, R. P. Eatough, B. Li, D. R. Lorimer, Y. Dai, Y. Li, X. Zhang, M. Li, T. Su, Y. Wu, Y. Pan, Y. Lian, T. Liu, Z. Yan, and Z. Pan, FAST Discovery of Eight Isolated Millisecond Pulsars in NGC 6517, *Astrophys. J. Lett.* **969**, L7 (2024), [arXiv:2405.18228 \[astro-ph.HE\]](#).
 - [13] Y. Wu, Z. Pan, L. Qian, S. M. Ransom, R. P. Eatough, B. Wang, P. C. C. Freire, K. Liu, Z. Yan, J. Luo, L. Zhang, M. Li, D. Yin, B. Li, Y. Li, Y. Dai, Y. Li, X. Zhang, T. Liu, and Y. Pan, The Discovery of Three Pulsars in the Globular Cluster M15 with FAST, *Astrophys. J. Lett.* **974**, L23 (2024), [arXiv:2312.06067 \[astro-ph.HE\]](#).
 - [14] Z. Pan, L. Qian, X. Ma, K. Liu, L. Wang, J. Luo, Z. Yan, S. Ransom, D. Lorimer, D. Li, and P. Jiang, FAST Globular Cluster Pulsar Survey: Twenty-four Pulsars Discovered in 15 Globular Clusters, *Astrophys. J. Lett.* **915**, L28 (2021), [arXiv:2106.08559 \[astro-ph.HE\]](#).
 - [15] S.-J. Gao, Y.-X. Shao, P. Wang, P. Zhou, X.-D. Li, L. Zhang, J. W. Kania, D. R. Lorimer, and D. Li, Discovery of a Millisecond Pulsar Associated with Terzan 6, *Astrophys. J. Lett.* **974**, L2 (2024), [arXiv:2409.10801 \[astro-ph.HE\]](#).
 - [16] Y. Lian, Z. Pan, H. Zhang, S. Cao, P. C. C. Freire, L. Qian, R. P. Eatough, L. Shao, S. M. Ransom, D. R. Lorimer, D. Yin, Y. Dai, K. Liu, L. Wang, Y. Wang, Z. Zhang, Z. Feng, B. Li, M. Li, T. Liu, Y. Li, B. Peng, Y. Pan, Y. Wu, L. Zhang, X. Zhang, and P. Jiang, The FAST Globular Cluster Pulsar Survey (GC FANS), [arXiv e-prints](#), [arXiv:2506.07970 \(2025\)](#), [arXiv:2506.07970 \[astro-ph.HE\]](#).
 - [17] A. Ridolfi, T. Gautam, P. C. C. Freire, S. M. Ransom, S. J. Buchner, A. Possenti, V. Venkatraman Krishnan, M. Bailes, M. Kramer, B. W. Stappers, F. Abbate, E. D. Barr, M. Burgay, F. Camilo, A. Corongiu, A. Jameson, P. V. Padmanabh, L. Vleschower, D. J. Champion, W. Chen, M. Geyer, A. Karastergiou, R. Karuppusamy, A. Parthasarathy, D. J. Reardon, M. Serylak, R. M. Shannon, and R. Spiewak, Eight new millisecond pulsars from the first MeerKAT globular cluster census, *Mon. Not. R. Astron. Soc.* **504**, 1407 (2021), [arXiv:2103.04800 \[astro-ph.HE\]](#).
 - [18] J. Das, J. Roy, P. C. C. Freire, S. M. Ransom, B. Bhattacharyya, K. Adamek, W. Armour, S. Kudale, and M. V. Muley, Globular Clusters GMRT Pulsar Search (GCGPS) I: Survey description, discovery and timing of the first pulsar in NGC 6093 (M80), [arXiv e-prints](#), [arXiv:2502.09154 \(2025\)](#), [arXiv:2502.09154 \[astro-ph.HE\]](#).
 - [19] S. Dai, S. Johnston, M. Kerr, F. Camilo, A. Cameron, L. Toomey, and H. Kumamoto, Discovery of Millisecond Pulsars in the Globular Cluster Omega Centauri, *Astrophys. J. Lett.* **888**, L18 (2020), [arXiv:1912.08079 \[astro-ph.HE\]](#).
 - [20] S. Dai, S. Johnston, M. Kerr, J. Berteaud, B. Bhattacharyya, F. Camilo, and E. Keane, Timing of pulsars in the globular cluster omega centauri, *Mon. Not. R. Astron. Soc.* **521**, 2616 (2023), [arXiv:2303.02834 \[astro-ph.HE\]](#).
 - [21] J. Hessels, A. Possenti, M. Bailes, C. Bassa, P. C. C. Freire, D. R. Lorimer, R. Lynch, S. M. Ransom, and I. H. Stairs, Pulsars in Globular Clusters with the SKA, in *Advancing Astrophysics with the Square Kilometre Array (AASKA14)* (2015) p. 47, [arXiv:1501.00086 \[astro-ph.HE\]](#).
 - [22] A. Askar, V. F. Baldassare, and M. Mezcua, Intermediate-Mass Black Holes in Star Clusters and Dwarf Galaxies, [arXiv e-prints](#), [arXiv:2311.12118 \(2023\)](#), [arXiv:2311.12118 \[astro-ph.GA\]](#).
 - [23] M. Mezcua, Observational evidence for intermediate-mass black holes, *International Journal of Modern Physics D* **26**, 1730021 (2017), [arXiv:1705.09667 \[astro-ph.GA\]](#).
 - [24] J. E. Greene, J. Strader, and L. C. Ho, Intermediate-Mass Black Holes, *Annu. Rev. Astron. Astrophys.* **58**, 257 (2020), [arXiv:1911.09678 \[astro-ph.GA\]](#).
 - [25] H. Baumgardt, J. Makino, and T. Ebisuzaki, Massive Black Holes in Star Clusters. II. Realistic Cluster Models, *Astrophys. J.* **613**, 1143 (2004), [arXiv:astro-ph/0406231 \[astro-ph\]](#).
 - [26] S. Lee, H. M. Lee, J.-h. Kim, R. Spurzem, J. Hong, and E. Chung, Formation and Evolution of Compact Binaries Containing Intermediate Mass Black Holes in Dense Star Clusters, [arXiv e-prints](#), [arXiv:2503.22109 \(2025\)](#), [arXiv:2503.22109 \[astro-ph.GA\]](#).
 - [27] M. Giersz, N. Leigh, A. Hypki, N. Lützgendorf, and A. Askar, MOCCA code for star cluster simulations - IV. A new scenario for intermediate mass black hole formation in globular clusters, *Mon. Not. R. Astron. Soc.* **454**, 3150 (2015), [arXiv:1506.05234 \[astro-ph.GA\]](#).
 - [28] L. Blecha, N. Ivanova, V. Kalogera, K. Belczynski, J. Fregeau, and F. Rasio, Close Binary Interactions of Intermediate-Mass Black Holes: Possible Ultraluminous X-Ray Sources?, *Astrophys. J.* **642**, 427 (2006), [arXiv:astro-ph/0508597 \[astro-ph\]](#).
 - [29] N. W. C. Leigh, N. Lützgendorf, A. M. Geller, T. J. Maccarone, C. Heinke, and A. Sesana, On the coexistence of stellar-mass and intermediate-mass black holes in globular clusters, *Mon. Not. R. Astron. Soc.* **444**, 29 (2014), [arXiv:1407.4459 \[astro-ph.SR\]](#).
 - [30] M. MacLeod, M. Trenti, and E. Ramirez-Ruiz, The Close Stellar Companions to Intermediate-mass Black Holes, *Astrophys. J.* **819**, 70 (2016), [arXiv:1508.07000 \[astro-ph.HE\]](#).
 - [31] M. Arca Sedda, P. Amaro Seoane, and X. Chen, Merging stellar and intermediate-mass black holes in dense clusters: implications for LIGO, LISA, and the next generation of gravitational wave detectors, *Astron. Astrophys.* **652**, A54 (2021), [arXiv:2007.13746 \[astro-ph.GA\]](#).
 - [32] S. Konstantinidis, P. Amaro-Seoane, and K. D. Kokkotas, Investigating the retention of intermediate-mass black holes in star clusters using N-body simulations, *Astron. Astrophys.* **557**, A135 (2013), [arXiv:1108.5175 \[astro-ph.CO\]](#).
 - [33] C.-J. Haster, F. Antonini, V. Kalogera, and I. Mandel, N-Body Dynamics of Intermediate Mass-ratio Inspirals in Star Clusters, *Astrophys. J.* **832**, 192 (2016), [arXiv:1606.07097 \[astro-ph.HE\]](#).
 - [34] M. A. Gürkan, J. M. Fregeau, and F. A. Rasio, Massive Black Hole Binaries from Collisional Runaways, *Astrophys. J. Lett.* **640**, L39 (2006), [arXiv:astro-ph/0512642 \[astro-ph\]](#).
 - [35] P. Amaro-Seoane and M. Freitag, Intermediate-Mass Black Holes in Colliding Clusters: Implications for Lower Frequency Gravitational-Wave Astronomy, *Astrophys. J. Lett.* **653**, L53 (2006), [arXiv:astro-ph/0610478 \[astro-ph\]](#).

- [36] M. Arca Sedda and A. Mastrobuono-Battisti, Mergers of globular clusters in the Galactic disc: intermediate mass black hole coalescence and implications for gravitational waves detection, *arXiv e-prints*, [arXiv:1906.05864 \(2019\)](#), [arXiv:1906.05864 \[astro-ph.GA\]](#).
- [37] A. Rasskazov, G. Fragione, and B. Kocsis, Binary Intermediate-mass Black Hole Mergers in Globular Clusters, *Astrophys. J.* **899**, 149 (2020), [arXiv:1912.07681 \[astro-ph.GA\]](#).
- [38] L. Souvatzis, A. Rantala, and T. Naab, The role of Massive Black Holes in merging star clusters: dynamical evolution, stellar & compact object ejections and gravitational waves, *Mon. Not. R. Astron. Soc.* **10.1093/mnras/staf458** (2025), [arXiv:2503.11813 \[astro-ph.GA\]](#).
- [39] M. V. Sazhin and M. V. Saphonova, Gravitational Action of Binaries on Pulsar Timing in Globular Clusters, *Astrophys. Space Sci.* **208**, 93 (1993).
- [40] R. Fakir, Detectable time delays from gravity waves?, *Phys. Rev. D* **50**, 3795 (1994), [arXiv:astro-ph/9306019 \[astro-ph\]](#).
- [41] A. N. Lommen, J. Bilkova, F. A. Jenet, S. Portegies Zwart, and B. W. Stappers, Using Pulsars to Detect Black Hole Binaries in Globular Clusters, in *Binary Radio Pulsars*, Astronomical Society of the Pacific Conference Series, Vol. 328, edited by F. A. Rasio and I. H. Stairs (2005) p. 225.
- [42] T. Damour and G. Esposito-Farèse, Light deflection by gravitational waves from localized sources, *Phys. Rev. D* **58**, 044003 (1998), [arXiv:gr-qc/9802019 \[gr-qc\]](#).
- [43] S. M. Kopeikin, G. Schäfer, C. R. Gwinn, and T. M. Eubanks, Astrometric and timing effects of gravitational waves from localized sources, *Phys. Rev. D* **59**, 084023 (1999), [arXiv:gr-qc/9811003 \[gr-qc\]](#).
- [44] A. D. Helfer, Light rays, gravitational waves and pulse-time offsets, *Mon. Not. R. Astron. Soc.* **430**, 305 (2013), [arXiv:1212.2926 \[gr-qc\]](#).
- [45] F. A. Jenet, T. Creighton, and A. Lommen, Pulsar Timing and the Detection of Black Hole Binary Systems in Globular Clusters, *Astrophys. J. Lett.* **627**, L125 (2005), [arXiv:astro-ph/0505585 \[astro-ph\]](#).
- [46] D. R. Madison, D. F. Chernoff, and J. M. Cordes, Pulsar timing perturbations from Galactic gravitational wave bursts with memory, *Phys. Rev. D* **96**, 123016 (2017), [arXiv:1710.04974 \[astro-ph.GA\]](#).
- [47] B. B. P. Perera, B. W. Stappers, A. G. Lyne, C. G. Bassa, I. Cognard, L. Guillemot, M. Kramer, G. Theureau, and G. Desvignes, Evidence for an intermediate-mass black hole in the globular cluster NGC 6624, *Mon. Not. R. Astron. Soc.* **468**, 2114 (2017), [arXiv:1705.01612 \[astro-ph.HE\]](#).
- [48] M. Häberle, N. Neumayer, A. Seth, A. Bellini, M. Li-bralato, H. Baumgardt, M. Whitaker, A. Dumont, M. Alfaro-Cuello, J. Anderson, C. Clontz, N. Kacharov, S. Kamann, A. Feldmeier-Krause, A. Milone, M. S. Nitschai, R. Pechetti, and G. van de Ven, Fast-moving stars around an intermediate-mass black hole in ω centauri, *Nature* **631**, 285–288 (2024).
- [49] Y. Huang, Q. Li, J. Liu, X. Dong, H. Zhang, Y. Lu, and C. Du, A high-velocity star recently ejected by an intermediate-mass black hole in M15, *National Science Review* **12**, 347 (2025), [arXiv:2406.00923 \[astro-ph.GA\]](#).
- [50] M. Anholm, S. Ballmer, J. D. E. Creighton, L. R. Price, and X. Siemens, Optimal strategies for gravitational wave stochastic background searches in pulsar timing data, *Phys. Rev. D* **79**, 084030 (2009), [arXiv:0809.0701 \[gr-qc\]](#).
- [51] B. J. Prager, S. M. Ransom, P. C. C. Freire, J. W. T. Hessels, I. H. Stairs, P. Arras, and M. Cadelano, Using Long-term Millisecond Pulsar Timing to Obtain Physical Characteristics of the Bulge Globular Cluster Terzan 5, *Astrophys. J.* **845**, 148 (2017), [arXiv:1612.04395 \[astro-ph.SR\]](#).
- [52] R. D. Blandford, R. W. Romani, and J. H. Applegate, Timing a millisecond pulsar in a globular cluster., *Mon. Not. R. Astron. Soc.* **225**, 51P (1987).
- [53] E. S. Phinney, Pulsars as Probes of Newtonian Dynamical Systems, *Philosophical Transactions of the Royal Society of London Series A* **341**, 39 (1992).
- [54] M. Maggiore, *Gravitational Waves: Volume 1: Theory and Experiments* (Oxford University Press, 2007).
- [55] P. C. Peters and J. Mathews, Gravitational Radiation from Point Masses in a Keplerian Orbit, *Physical Review* **131**, 435 (1963).
- [56] A. Bañares-Hernández, F. Calore, J. M. Camalich, and J. I. Read, New constraints on the central mass contents of Omega Centauri from combined stellar kinematics and pulsar timing, *arXiv e-prints*, [arXiv:2408.00939 \(2024\)](#), [arXiv:2408.00939 \[astro-ph.GA\]](#).
- [57] J. Gerssen, R. P. van der Marel, K. Gebhardt, P. Guhathakurta, R. C. Peterson, and C. Pryor, Hubble Space Telescope Evidence for an Intermediate-Mass Black Hole in the Globular Cluster M15. II. Kinematic Analysis and Dynamical Modeling, *Astron. J.* **124**, 3270 (2002), [arXiv:astro-ph/0209315 \[astro-ph\]](#).
- [58] H. Baumgardt, P. Hut, J. Makino, S. McMillan, and S. Portegies Zwart, On the Central Structure of M15, *Astrophys. J. Lett.* **582**, L21 (2003), [arXiv:astro-ph/0210133 \[astro-ph\]](#).